Large strain theory applied to self-gravitating bodies: A numerical approach

Wolfgang H. Müller, Wolf Weiss
wolfgang.h.mueller@tu-berlin.de

Abstract

This paper presents an analysis of the deformation in terrestrial objects, such as the inner planets, rocky moons, or asteroids, which is due to self-gravitation. The problem of modeling such structures is quite old and goes back to the work of Kelvin, Rayleigh, Love, and Jeans in the late 1800. In those days a linear-elastic, closed-form solution was presented and studied. However, it turns out that in the case of huge objects, such as Earth or Venus, the resulting strains can become quite large. Thus, in the sixties, non-linear elasticity was used and large strains were taken into account. The conclusion was that some crucial parameters, *e.g.*, the location of the Love radius, do not change much when switching from the linear to the non-linear regime. However, this is true only for certain choices of effective stiffness parameters for the celestial body. At that time this was difficult to see, because the non-linear analysis is based on numerical solution procedures, which were less developed back then.

In this paper we will first present some of the history of the problem, then show the breakdown of the linear-elastic solution and, finally, use modern continuum mechanics tools to derive the underlying non-linear equations. We will solve them by applying two numerical techniques, namely Runge-Kutta methods for the solution of differential equation as well as finite differences.

At the end we will discuss the limits of the numerical approaches and present an outlook to further alternatives.

1 Introduction and problem statement

The problem of modeling the deformation, *i.e.*, the displacements, stresses and strains in self-gravitating terrestrial bodies by suitable constitutive equations for solids is quite old. In what follows we will restrict ourselves to homogeneous solid spheres, so that the problem reduces to a fully radially symmetric case. First attempts at finding such solutions were based on the linear theory of elasticity, *i.e.*, on the combination of the static balance of momentum with Hooke's law, formulated at small strains. A rather extensive exposition of this problem for a constant, homogeneous mass density, including also the effects of centrifugal forces, can be found in [1]. A corresponding analytical result for the radial displacement is presented in [2], Sect. 98. Most recently, results for this problem have been summarized resulting in concise formulae in [3]. The differential equation for the radial displacement in

the linear small strain case reads (dashes denote differentiations w.r.t. the radius, r, $G = 6.67410^{-11}\mathrm{m}^3\mathrm{kg}^{-1}\mathrm{s}^{-2}$ is the gravitational constant, ρ_0 is the (constant) mass density, $\lambda = \frac{E\nu}{(1-2\nu)(1+\nu)}$, $\mu = \frac{E}{2(1+\nu)}$ are Lamé's constants, E and ν are Young's modulus and Poisson's ratio, respectively):

$$u_r'' + 2\frac{u_r'}{r} - 2\frac{u_r}{r^2} = \frac{4\pi G\rho_0^2}{3(\lambda+2\mu)}r, \tag{1}$$

and its solution is given by:

$$u_r = -\frac{\alpha_k}{30}\frac{1+\nu}{1-\nu}\left(\frac{3-\nu}{1+\nu} - \frac{r^2}{r_0^2}\right)r, \quad \alpha_k = \frac{4\pi G\rho_0^2 r_0^2}{3k}. \tag{2}$$

where $k = \frac{E}{3(1-2\nu)}$ is the (homogenized, *i.e.*, effective) bulk modulus of the terrestrial body (a.k.a. elastic modulus of compressibility), and r_0 denotes the outer radius. This relation can be used to determine the position where the radial strain changes sign. This was first done in [2] where it was found that:

$$r_{\mathrm{Love}} = r_0\sqrt{\frac{3-\nu}{3(1+\nu)}}. \tag{3}$$

The radial strain is of tensile nature above this position and compressive below. Note that the circumferential strain is always compressive. Love did not say if he intended this quantity to be more than just a curiosity. We may speculate that the tensile nature of a principal strain could be used in context with a damage criterion, but we will not discuss this any further in this paper. Eqn. (2) was used to calculate the strain on the surface for various terrestrial bodies based on data compiled in [3], as a function of varying effective compressibility. The latter is hard to specify in each particular case, especially since the planets are not completely solid. Therefore, a range of reasonable values for k should be examined. The results are shown in Fig. 1. On the left we see plots for the inner planets (Mercury and Mars in red and dashed-black, respectively, nearly coinciding, Venus in green, and Earth in blue). On the right we see results for Earth's Moon (red), Io (green), Europa (blue), Ganymede (black), Callisto (magenta), and Titan (cyan). For the moons, Mercury, and Mars the strains are small enough in order to accept linear small strain elasticity as a viable tool for computing the deformation. In the case of Venus and of Earth the strains are *not* small. Rather they turn out to be of the order of 10 percent and more, which is alarmingly high, to say the least.

Thus, in the sixties there was a revival of the problem. First, because based on seismic measurements more complex models of the density distribution of the Earth became available, *e.g.*, [4], [5], and, second, because of the conclusion that linear strain theory might be insufficient to describe the situation in rather massive terrestrial bodies. This concern was expressed explicitly in [6] and [4]. This analysis was based on the paper by Seth [7] on finite elasticity, which operates in current space, uses the Eulerian-Almansi tensor as a strain measure, and related it to the current Cauchy stress in terms of a quasi Hookean equation. The numerical approach used infinite series for a displacement related quantity in context with a corresponding

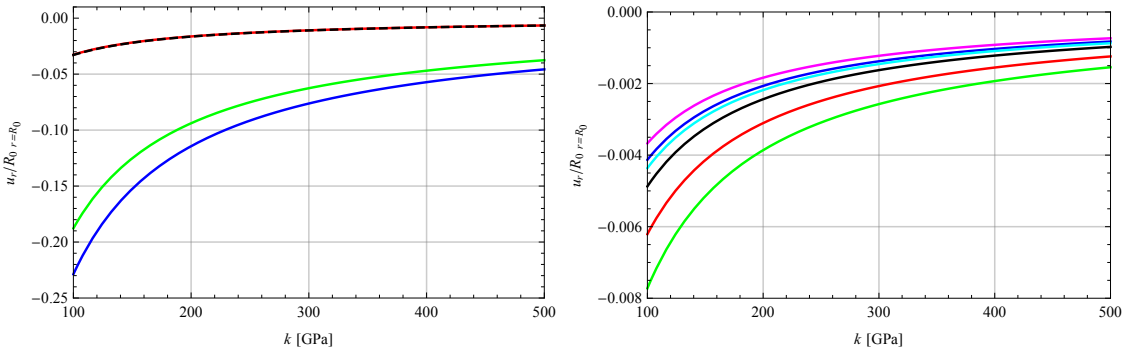

Figure 1: Strains on the periphery of various terrestrial bodies as a function of effective compressibility (for color code see text).

highly linear differential equation stemming from the static equation of momentum in the current configuration together with empirically motivated equations for the mass density and the corresponding self-gravitating force field. We will elaborate on this in the next section.

2 The governing equations in the nonlinear case

We consider the purely radially symmetric case of self-gravitation for a sphere with a homogeneous mass density ρ_0 in the unstressed reference configuration, $\mathcal{B}_0$. In fact, just like the effective compressibility, k, this is a parameter, which is relatively hard to assess. Indeed, frequently we do know the total mass, m, of a terrestrial object. However, we do not know its outer radius R_0 before gravity has been "switched on," so-to-speak. Therefore, the equation $\rho_0 = \frac{m}{\frac{4\pi}{3}R_0^3}$ cannot directly be used to determine the reference mass density. However, we shall see later that ρ_0 and the effective elastic parameters of the terrestrial object in question form a dimensionless factor, α. It is this factor we will vary within reasonable bounds, since the effective elastic parameters are just as elusive as the mass density of the reference configuration.

It is for such reasons that it is useful to formulate the continuum mechanics equations w.r.t. the current configuration, $\mathcal{B}(t)$, and *not* w.r.t. $\mathcal{B}_0$. This contradicts to a certain degree standard procedures of modern continuum mechanics, which has a certain preference for the use of the reference configuration in terms of a full description in material space. It is interesting to note that the need for the concept of a reference configuration for self-gravitating bodies was anticipated quite early in the papers of Jeans [8] and Lord Rayleigh [9], respectively. It has also received further attention more recently, *e.g.* in [10]. However, as indicated above, this is a treacherous way to go, at least from a practical point-of-view, since the outer radius of an undeformed planet is not a directly measurable quantity. With this in mind we will start from the static balance of momentum in *current* spherical coordinates. In the totally radially symmetric case only the radial component is different from zero and reads (*cf.*, [11], pg. 116, σ_{ij} denote the Cauchy stresses in spherical coordinates):

$$\frac{\mathrm{d}\sigma_{rr}}{\mathrm{d}r} + \frac{2\sigma_{rr} - \sigma_{\vartheta\vartheta} - \sigma_{\varphi\varphi}}{r} = -\rho f_r\,,\ \rho = \frac{\rho_0}{\det \boldsymbol{F}}\,,\ f_r = -\frac{Gm(r_0)}{r^2}. \tag{4}$$

In the present case it is reasonable to make the ansatz $r = r(R) \Leftrightarrow R = R(r)$ for the deformation (r refers to the current radial and R to the radial position in the reference configuration, respectively). Hence the deformation gradient, $\boldsymbol{F}$, and the Euler-Almansi strain tensor, $\boldsymbol{e}$, read in spherical coordinates:

$$\boldsymbol{F} = \begin{pmatrix} \frac{\mathrm{d}r}{\mathrm{d}R} & 0 & 0 \\ 0 & \frac{r}{R} & 0 \\ 0 & 0 & \frac{r}{R} \end{pmatrix} \;\Rightarrow\; 2\boldsymbol{e} = \begin{pmatrix} 1-\left(\frac{\mathrm{d}R}{\mathrm{d}r}\right)^2 & 0 & 0 \\ 0 & 1-\left(\frac{R}{r}\right)^2 & 0 \\ 0 & 0 & 1-\left(\frac{R}{r}\right)^2 \end{pmatrix}. \tag{5}$$

From Eqn. $(5)_1$ we find immediately that $\det\boldsymbol{F}^{-1} = \frac{\mathrm{d}R}{\mathrm{d}r}\left(\frac{R}{r}\right)^2$. Moreover, the form of the body force in Eqn. (4) deserves a comment: At the current position r of a sphere with an exclusively radial mass density distribution, $\rho(r)$, the attraction is directed toward the center and dictated by the total mass, $m(r)$, situated beneath this position. However, due to mass conservation we have $m(r) \equiv m(R) = \frac{4\pi}{3}\rho_0 R^3$. In this context it should be noted that Eqn. $(4)_3$ is a direct and exact consequence of Poisson's equation for the potential, U, in case of a radially symmetric mass distribution, $\rho(r)$:

$$\frac{1}{r^2}\frac{\mathrm{d}}{\mathrm{d}r}\left(r^2\frac{\mathrm{d}U}{\mathrm{d}r}\right) = 4\pi G\rho(r) \;\Rightarrow \tag{6}$$

$$f_r \equiv -\frac{\mathrm{d}U}{\mathrm{d}r} = -\frac{4\pi G}{r^2}\int_{r=0}^{r=r_0} r^2\rho(r)\mathrm{d}r \equiv -\frac{Gm(r_0)}{r^2}.$$

We now turn to the constitutive equation for the stress-strain relations. Following [7], pg. 234 these are given by Hooke's law where the linear strains, ε_{ij}, have been replaced by the nonlinear ones, e_{ij}, $j \in r, \vartheta, \varphi$. Therefore the non-vanishing Cauchy stress components, σ_{ij}, read:

$$\sigma_{rr} = (\lambda+2\mu)\,e_{rr} + \lambda(\,e_{\vartheta\vartheta} + e_{\varphi\varphi}\,),\;\; \sigma_{\vartheta\vartheta} \equiv \sigma_{\varphi\varphi} = 2(\lambda+\mu)\,e_{\vartheta\vartheta} + \lambda\,e_{rr}. \tag{7}$$

If Eqns. (4)-(6) are inserted into each other a nonlinear differential equation of second order for $r(R)$ results, which can be rewritten in terms of the radial displacement $u_r(r) \equiv r - R(r)$. It is instructive to convince oneself that this equation reduces to Eqn. (1) of the linear case if all nonlinear terms are neglected. Clearly, the nonlinear differential equation must be analyzed numerically. For this purpose it is useful to, first, change to dimensionless coordinates by normalizing the current radius with the current outer radius, r_0, so that $x = r/r_0$ and $u(x) = u_r/r_0$. Second, following [6], we introduce an auxiliary quantity, $\beta(x)$, by $R(r) = r\beta(r) \;\Rightarrow\; u_r(r) = r[1-\beta(r)]$. This will prove to be beneficial during the numerical analysis. Hence, we arrive at:

$$\frac{\mathrm{d}}{\mathrm{d}x}\left[3\beta^2 + \left(\beta'^2 + \frac{2\beta\beta'}{x}\right)x^2\right] + \frac{2(1-2\nu)}{1-\nu}x\beta'^2 = -\alpha(\beta + x\beta')\beta^5 x, \tag{8}$$

where the factor $\alpha = \frac{8\pi G\rho_0^2 r_0^2}{3(\lambda+2\mu)}$ has been introduced, which bears a certain similarity to the one in Eqn. $(1)_2$. Both differential equations are of second order and need two boundary conditions for their analytical or numerical treatment, respectively. In the case of Eqn. (8) these result from the requirement that the (normalized) radial displacement, $u(x)$, must be an odd function in x, *i.e.*, $\beta'(0) = 0$. Moreover, the surface of the sphere is traction-free, *i.e.*, $\sigma_{rr}|_{r=r_0} = 0$, which is equivalent to $\frac{1+\nu}{1-\nu}\left[1-\beta^2(1)\right] - \left[\beta'^2(1) + 2\beta(1)\beta'(1)\right] = 0$.

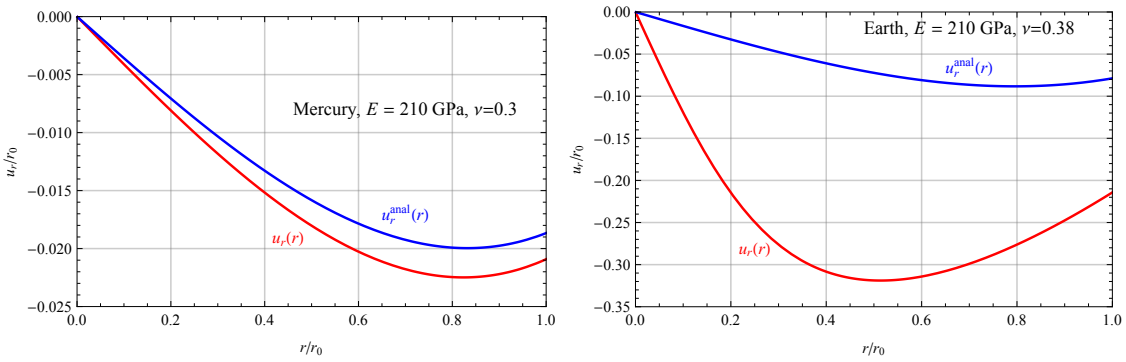

Figure 2: Radial displacement as a function of radial position.

3 Numerical analysis and discussion

At the beginning of this section it should be mentioned that in the work by Bose and Chattarji [6] and Pan [4] a solution for $\beta(x)$ was sought in form of a Taylor power series. In fact, this is a very tedious and sometimes inaccurate approach, in particular, if more complex density distributions are studied. The latter affect directly the right hand side of Eqn. $(4)_1$. In fact, these authors insert highly nonlinear expressions for ρf_r, because they want to model the impact of Earth's heterogeneous mass distribution.

Interestingly $\rho(r)$ and $f_r(r)$ are given in separate, but related[†] equations based on some earlier work by Bolt [12]. The right hand side of Eqn. (8) is highly linear, too, despite the fact that the reference density is homogeneous. Clearly, our current density is not homogeneous because of Eqn. $(4)_2$. However, in contrast to the previous authors, it is not neither phenomenological nor assumed. Rather it is a straightforward continuum mechanics result from the assumption of a *single* reference mass density. In other words, the current distribution of the mass density can be calculated once we have solved the boundary value problem for $\beta(x)$. Moreover, f_r is nonlinear because of the nonlinearity inherent to Eqn. $(4)_3$. It is an *exact* expression for purely radial mass density distributions, $\rho(r)$, and that is all there is to it.

We now turn to a numerical solution of Eqn. (8). The first technique to be used is based on the NDSolve command from Mathematica ([13]). NDSolve is based on Runge-Kutta integration techniques for ODEs. In addition we used the option "stiffness switching," since Eqn. (8) reacts in a stiff manner, due to its inherent singularity at $r = 0$ or $x = 0$. The latter is already present in the linear case described by Eqn. (1). However, there it can simply be excluded by putting the corresponding constant of integration in the analytical solution equal to zero. Moreover, it should be pointed out that despite this optional choice, we were not able to obtain a solution for the proper boundary condition $\beta'(0) = 0$. Rather we had to choose $\beta'(\epsilon) = 0$ with $\epsilon = 10^{-3}$.

Two results are shown in Fig. 2. For the plots geometry and mass data for Mercury and Earth were chosen from [3]. It should be pointed out that ρ_0 was

[†]by Newton's gravitational principle

estimated by using the relation $\frac{m}{\frac{4\pi}{3}r_0^3}$, *i.e.*, the current outer radius of the planets. In the case of Mercury the values of iron were chosen for Young's modulus and Poisson's ratio, leading to $\alpha \approx 0.35$. If the same elastic data was used for Earth α increased up to 1.96. For this value convergence could no longer be obtained. Hence, Poisson's ratio was raised to 0.38, which is equivalent to $\alpha \approx 1.75$. The reason for the lack of convergence becomes apparent by looking at the plots: In the case of Mercury, there is already a slight discrepancy to the analytical solution, $u_r^{\mathbf{anal}}(r)$, shown in Eqn. $(2)_1$. The analytical solution *underestimates* the displacement. This is not surprising since a radial strain, which is roughly given by u_r/r_0, of more than two percent is already testing the limits of a linear theory.

In the case of Earth the situation is much more dramatic. First, the difference between the analytical and the numerical solution is huge and, second, even the analytical solution already predicts strains of almost 10%, whereas the numerical solution amounts to 30% and more. Note that the curvature of $u_r(r)$ "on the left" becomes more and more pronounced when the α-values increase. For large values of α, *i.e.*, for large values of reference density and small values of Young's modulus and/or Poisson's ratio, the $u_r(r)$-curve will first decline very steeply and then show an essentially linear behavior with a moderate slope. Such extreme gradients with kinks are very difficult to master numerically.

It is for this reason that we now turn to a potentially alternative numerical method, namely a finite-difference scheme. Eqn. (8) is transformed into a set of non-linear coupled equations, resulting in a sparsely populated matrix, by approximating the solution in discrete points, $i = 1..., i_{\max}$ on the interval $x \in [0, 1]$ separated by the distance Δx. "In the flesh" we use finite difference approximations of $\mathcal{O}(\Delta x^2)$ for the first and second order differential quotients as follows:

$$\beta'(x) \approx \frac{\beta(i+1) - \beta(i-1)}{2\Delta x}\,,\ \beta''(x) \approx \frac{\beta(i-1) - 2\beta(i) + \beta(i+1)}{\Delta x^2}. \tag{9}$$

At the left and right hand side of the $[0, 1]$-interval we use for the first derivatives with the same degree of accuracy:

$$\beta'(0) = \frac{-3\beta(1) + 4\beta(2) - \beta(3)}{2\Delta x} + \mathcal{O}(\Delta x^2), \tag{10}$$

$$\beta'(1) = \frac{\beta(i_{\max} - 2) - 4\beta(i_{\max} - 1) + 3\beta(i_{\max})}{2\Delta x} + \mathcal{O}(\Delta x^2).$$

Some results are shown in Fig. 3. The plots on the left show that the finite difference method leads to exactly the same results of the NDSolve command, at least as long as the parameter α does not reach a certain threshold. This is explored in the plots on the right. Recall that $\nu = 0.38$, $E = 210$ MPa with Earth parameters, *i.e.*, $\alpha \approx 1.75$ was the convergence limit in case of NDSolve. The finite difference technique allows to go a little beyond this value up $\nu = 0.37$, *i.e.*, $\alpha \approx 1.86$. The plots show that an increasing value of α leads to an increase of strain, as anticipated. Moreover, the initial slope of the displacement curves increases rapidly. Then, at larger values of r/r_0, the displacement shows a more or less linear behavior. If we keep increasing α the transition zone is governed by huge gradients and turns

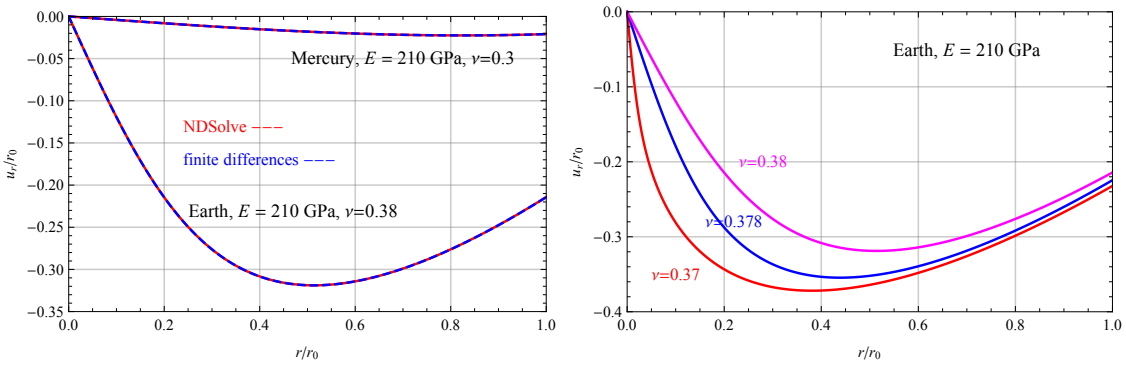

Figure 3: Finite difference vs. Runge-Kutta method.

essentially into a kink. However, this is very hard to capture numerically. In fact, the finite difference method fails to converge above the afore-mentioned α value. It might be an alternative to use a non-equidistant discretization. However, this is left to future research. Moreover, another numerical alternative might be to use finite elements. This will be explored in these proceedings in the paper by Müller and Lofink.

The curves in Fig. 3 also indicate that the position of the Love radius, *i.e.*, the position of the minimum of the u_r-curves, as predicted by the analytical solution shown in Eqn. (3) will change in the case of massive terrestrial objects. This is explored in detail in the plots of Fig. 4. The left inset presents three curves. First, the dependence of the Love radius according to Eqn. (3), which is labeled as the "analytical solution." Second, the plot called "Mercury," for which mass and geometry data of Mercury were used. Moreover, Young's modulus was that of iron, Poisson's ratio varied within the possible bounds, and the NDSolve command was applied to find a numerical solution of the nonlinear boundary-value problem. Thus, α-values changed between 0.47 and 0, when ν increased from 0 to 0.5. The result confirms the statements in [6] or [4] according to which the location of the Love radius is hardly affected by the nonlinear treatment of the deformation problem. However, this is only true, if α stays small, which is not guaranteed for a large object, such as Earth. This is shown in the third plot of Fig. 4 (left). In this case α varied between 0 and 1.75 when ν decreased from 0.5 to 0.38. Obviously, the difference to the analytical solution can become very large.

In summary, the location of the Love radius depends on *two* parameters, Poisson's ratio (which is the *only* parametric dependence in the analytical solution) *and* the mass-stiffness parameter, α. The plot on the right hand side of Fig. 4 explores this in more detail: The Love radius is plotted *vs.* α for various values of ν. The corresponding values for the Love radius according to the analytical solution are indicated by circles. They are valid for small values of α.

We now turn to the assessment of the redistribution of density due to the deformation. The non-linear numerical analysis is based on Eqn. $(4)_2$, which leads us to conclude that:

$$\frac{\rho}{\rho_0} = [\beta(x) + x\beta'(x)]\beta^2(x). \tag{11}$$

In the case of the analytical solution from Eqn. (2) we may write:

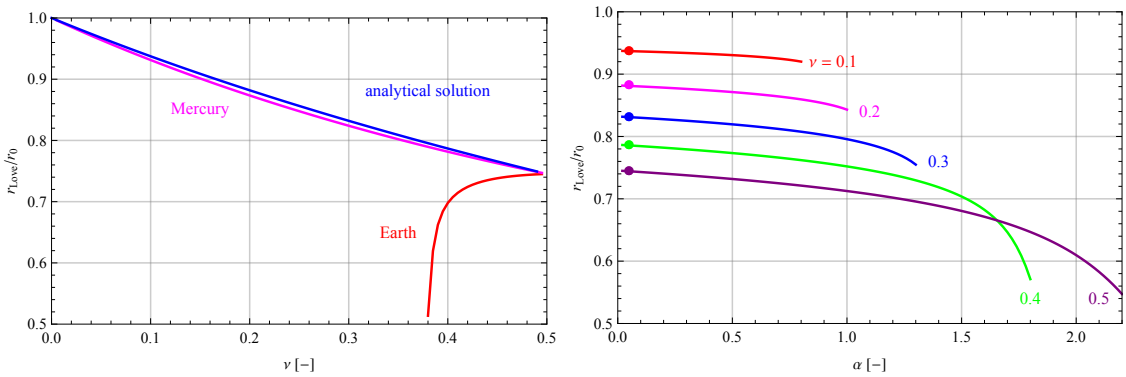

Figure 4: Position of the Love radius (see text).

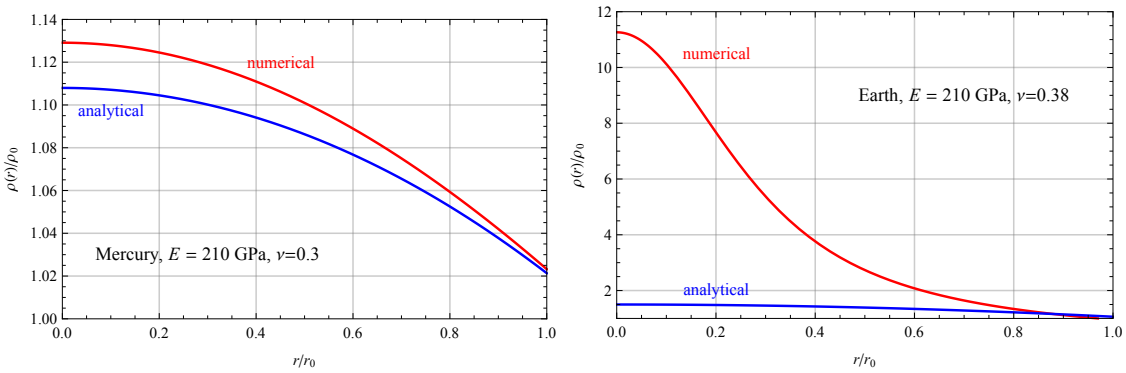

Figure 5: Normalized distribution of mass density predicted.

$$\frac{\rho}{\rho_0} = 1 - u_r'(x) - 2\frac{u_r(x)}{x}. \tag{12}$$

Fig. 5 shows results obtained by evaluating both equations. Clearly, the mass density increases toward the center of a planet even if the reference mass density is homogeneous and constant. In the case of a small planet (like Mercury) the density distributions from both equations are relatively close together. In the case of a large planet (like Earth) the numerical, *i.e.*, the solution from the non-linear equation of deformation leads to densities at the center much larger than those obtained from the linear solution. In other words: The nonlinearity allows us to understand and potentially model the dramatic increase of mass density in the center of massive terrestrial planets without assuming a denser core to begin with.

As a matter of fact, the increase in mass density shown on the right hand side of Fig. 5 is much too large. This is due to the assumption that the effective elasticity of Earth is essentially that of iron, which it is *not*, *and* that the Earth was homogeneous in the beginning when it formed, which it was certainly *not*. Indeed, the plot is intended to demonstrate the potential of a nonlinear description of deformation, a fact which, to the best knowledge of the authors, has not been emphasized in the literature so far. Indeed, the density distribution of the PREM model [14] are phenomenologically based on seismic measurements which were analyzed by using

(anisotropic) linear elasticity. All we wish to say at this point is that modeling the density distribution of Earth should be attempted in combination with a nonlinear deformation theory.

4 Summary and conclusion

In this paper we have analyzed the deformation in self-gravitating, initially homogeneous, solid spheres. An analytical solution valid for linear, small strain theory was juxtaposed to a numerical one of the corresponding boundary-value problem based on nonlinear, elastic, large strain theory. Problems in context with the numerical treatment of the nonlinear equation were discussed. It turns out that two dimensionless parameters govern the deformation problem, first, Poisson's ratio, ν, and, second, a mass-stiffness parameter, $\alpha = \frac{8\pi G\rho_0^2 r_0^2}{3(\lambda+2\mu)}$, characteristic of a particular sphere, *i.e.*, terrestrial planet. Presently, convergence of the numerical solution can only be guaranteed within a certain range of α. Further investigations, based on adaptive meshing techniques, are currently underway to expand this range. However, it can already be said that in contrast to previous statements in the literature, the location of the Love radius, *i.e.*, the transition between compressive to tensile radial strains within the sphere, is affected if nonlinear is used *and* the body in question is sufficiently massive and not too stiff.

Acknowledgements

The authors are grateful to Dr. Joydev Chattopadhyay, Editorial Secretary of the Calcutta Mathematical Society for providing us with a copy of the paper by [6].

References

[1] L. M. Hoskins. "The strain of a gravitating, compressible elastic sphere". In: *Trans. Amer. Math. Soc.* 11 (1910), pp. 203–248.

[2] A. E. H. Love. *A treatise on the mathematical theory of elasticity. Fourth edition.* Cambridge University Press, 1927.

[3] W. H. Müller and P. Lofink. "The movement of the Earth: Modeling of the flattening parameter". In: *Lecture Notes of TICMI, in print* (2015).

[4] S. K. Pan. "Deformation and stresses in different Earth models with a rigid core having varying elastic parameters". In: *Geofisica pura e applicata* 568.1 (1963), pp. 39–52.

[5] B. S. Samanta. "Stresses in different rotating spherical Earth models with rigid core". In: *Pure and applied geophysics* 63.1 (1966), pp. 68–81.

[6] S. C. Bose and P. P. Chattarji. "A note on the finite deformation in the interior of the Earth". In: *Bull. Calcutta Math. Soc.* 55.1 (1963), pp. 11–18.

[7] B. R. Seth. "Finite strain in elastic problems". In: *Phil. Trans. R. Soc. Lond. A.* 234 (1935), pp. 231–264.

[8] J. H. Jeans. “On the vibrations and stability of a gravitating planet”. In: *Phil. Trans. R. Soc. Lond. A* 201 (1903), pp. 331–345.

[9] O. M. Lord Rayleigh. “On the dilatational stability of the Earth”. In: *Proceedings of the Royal Society of London* 77.519 (1906), pp. 486–499.

[10] R. J. Geller. “Elastodynamics in a laterally heterogeneous, self-gravitating body”. In: *Geophysical Journal* 94 (1988), pp. 271–283.

[11] W. H. Müller. *An expedition to continuum theory*. Springer, 2014.

[12] B. A. Bolt. “Earth models with continuous density distribution”. In: *Geophysical Supplements to the Monthly Notices of the Royal Astronomical Society* 7.6 (1957), pp. 360–368.

[13] Wolfram. *Mathematica*. Wolfram Research, Inc., 2014.

[14] A. M. Dziewonski and D. L. Anderson. “Preliminary reference Earth model”. In: *Physics of the Earth and Planetary Interiors* 25 (1981), pp. 297–356.

Wolfgang H. Müller and Wolf Weiss, Technische Universität Berlin, Institute of Mechanics, Einsteinufer 5, D-10587 Berlin, Germany